Polychrome enamels, ceramics, glasses and their degradation

Ph Colomban

4.5 Polychrome enamels, ceramics, glasses and their degradation

Ph. Colomban,[a]*

[a] Sorbonne Université, CNRS, MONARIS UMR8233, 4 Place Jussieu, 75005 Paris, France

*Corresponding contributor. E-mail: philippe.colomban@sorbonne-universite.fr

ABSTRACT

Due to the good chemical stability of chemical bonds forming silicates, glass and pottery are generally well preserved and can be used as dating milestones. After a brief recall of the preparation of (glazed/enamelled) pottery and glass (utensils, stained glass windows) from the technical and historical points of view, the main chemical and physical characteristics of the glassy materials (composition, mechanical and thermal characteristics, porosity, etc.) are presented and discussed in relation to corrosion resistance. The corresponding analytical techniques are addressed. Emphasis is given on the different mechanisms of degradation (surface and bulk corrosion, crazing/peeling, proton/water insertion, lixiviation, oxidation) as well as conservation and restoration practices. Dating/authentication of ancient artefacts by the measurement of Raman signal at the surface of glassy silicates is further presented.

4.1 Definitions

Pottery, glass and enamelled artefacts are made of silicon- and aluminium-rich inorganic matter, namely the silicates which are the main constituents of the earth. These artefacts are made by thermal treatment of powdered rocks/minerals, such as sands, clays, feldspars and calcareous stones.[1-8] The silicate structure consists of the association of SiO_4 tetrahedron with AlO_4 or FeO_4 tetrahedron, AlO_6 or FeO_6 octahedron and similar chemical units in between which isolated ions may be located.[5,6] These structures can be crystalline or glassy. While glass is obtained by full/complete melting of the raw materials shaped at high temperature, using the controlled viscosity of molten glass, pottery is shaped before heating in the 'green' state taking advantage of the plasticity of humid clay mixture in which grains will be cemented and welded by firing. Enamels are any kind of glassy coatings (Fig.1) deposited and fired on a substrate (ceramic, glass or metal), already fired or in green state. A coating on pottery is called glaze. All processes involve powdering the raw materials in order to promote their reaction and homogenisation on heating. Due to the huge stability of Si-O and Al-O bonds, heating at high temperature is required to break and constitute the bonds again (sintering) and/or form new phases by reaction (dissolution-precipitation): temperatures ranging between 500°C and 1400°C are usually needed for silicates.[7] Higher temperatures may be required for advanced non-silicate technical ceramics and glasses. Achievement of a non-porous ceramic body usually requires temperatures higher than 1100-1200°C and total melting may typically occur between 600°C (lead-rich silicate) and 1500°C (flux-poor silicate), depending on the exact composition.[7-9] Consequently, ceramic, glass and enamel wares are very stable and well preserved for millennia and thus used to date archaeological layers. For instance, in African tropical countries where the preservation of carbon-based artefacts is difficult, dating of an archaeological layer is based on a specific pattern of pottery decor as well as the use of trade beads coming from the main places of production (chronologically Mesopotamia, Egypt and the Mediterranean world, India-South/East Asia, China and Europe) through particular routes (Indian Ocean and Monsoon wind shipping , trans-African terrestrial network).[10-11] Similarly, the habit and typology of tools made of natural silicates (obsidian, flint, cherts, cornelian, etc.) allow the dating of prehistorical archaeological contexts.[12,13]

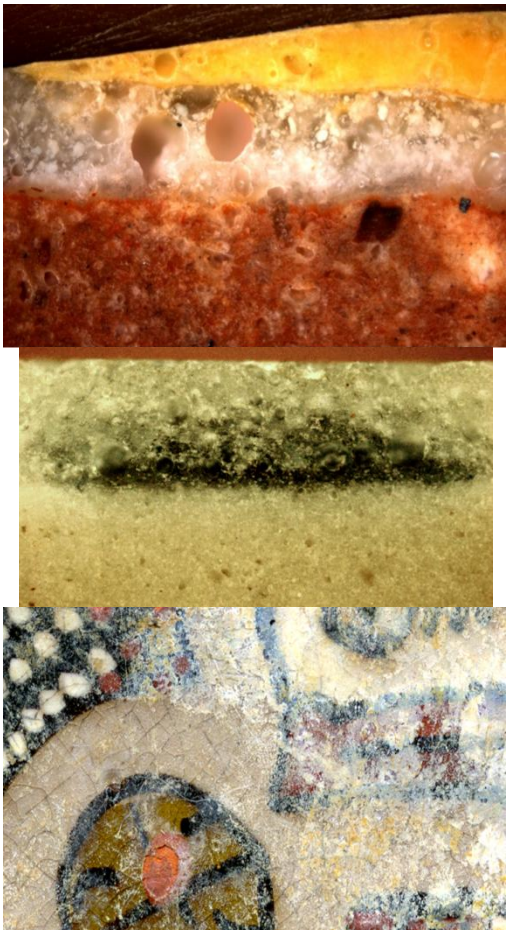

Figure 4.1 *Examples of glassy coatings deposited on a ceramic body; top, Naples yellow pigment coloured overglaze deposited on a colourless glaze layer (porous terra cotta body covered with ~300 µm double layer of glaze); centre, underglaze blue cobalt-based decor drawn on the green porcelain body and then body and glaze are fired simultaneously (glaze layer ~500 µm); bottom-right, example of surface corroded lead-based glaze (15x30 mm). Corrosion layers are very thin and require high magnification techniques to be studied.*

The degree of reaction in between the grains of silicate-based ceramics such as terra cotta, faience and fritware, i.e. those fired at low to medium temperature, is limited: most of the grains are not modified and the reaction takes place merely at their periphery .[14,15] Reactions are almost complete for stoneware and porcelain, both sintered above 1200°C. The main characteristic of a ceramic body is thus its heterogeneity. The grain size typically ranges between micron (phases formed by reaction) and millimetre (un- or partly-reacted raw materials). The core of the biggest grains is not transformed and may be subject to corrosion.[14-16] It is worth noting that a combination of analytical techniques is always needed for identifying the entire phases present in the ceramic body.[17,18] Amorphous phases cannot be identified by XRD while Raman spectroscopy also fails to detect the ionic phases. On the contrary, the homogeneity of colourless or slightly coloured glasses and enamels is very high since these materials are amorphous (glassy). The heterogeneity of these materials is at the lowest level, at the scale of the inter-atomic distances (the chemical bond ranges between 0.1 to 1 nm, Fig. 3). It is related to the degree of connectivity of the silicate network made of SiO_4 tetrahedron, with additional distribution of cations compensating the electric charge. Welding adjacent grains of a silicate ceramic body is achieved with the formation of a (temporary) liquid phase which wets the grain surface during firing and promotes reactions, dissolution-recrystallisation and formation of solid cement on cooling.[6,14,15] Enamels are coloured with transition metals or lanthanide ions or by dispersing /crystallizing an already coloured phase, namely a pigment.[16,19] Typically, 0.1 %wt of a colouring element (Co, Cu, Fe, etc.) is sufficient to colour glass.[19] A thin glaze layer requires a higher content of colouring phase and glass with a high volume of pigment/opacifier becomes a glass-ceramic with improved mechanical properties.[19,20]

4.2 Pottery, glass and enamelled artefacts: a brief historical overview

The mastering of fire is associated with the early development of mankind.[21] The first examples of pottery date as early as 12000 BC in Japan, Siberia and Africa, before or just at the Neolithic transition from nomadic to sedentary life. The deposit of a coating in the form of glassy silicates called 'enamel' or 'glaze', on stone (e.g. quartzite in Egypt) or ceramic substrate only started many millennia after the development of urban culture/elite in Egypt and Mesopotamia in ca. 1500 BC. The preparation of an artefact with glassy paste is a little older (> 2000 BC). The oldest enamel-on-metal wares date back to at least 1500 BC in Cyprus and 1100 BC in China. Glass and pottery were already being industrially produced at the times of the Roman Empire (>~50 BC) in rare places but were exported in the entire Roman world and abroad, up to Vietnam and China.[22] Chinese Eastern Han to Sui potters (2nd century BC to 7th century AD) initiated high-temperature firing technology, thanks to the building of advanced kilns. Temperatures higher than 1300°C were being achieved as early as the 3rd century AD. Consequently, white porcelains fired at high temperatures in advanced kilns appeared during the Sui and Tang Dynasties (7th-8th centuries AD). At the same time, Islamic potters of Bassrah and Mesopotamia found how to produce 'white' artefacts with complex depictions in competition with porcelain, using the Roman glassmaking technique of opacification by tin oxide in combination to low-temperature firing (< 1000°C) of a porous, common 'terra cotta' body made of fine clays or silts .[1,21,23,24] The technique spread around the Mediterranean Sea with the expansion of the Islamic world, namely Ifriqiya (7th c.), Al-Andalus (8th c.), Sicily (9th c.), Italy (majolica, 13th c.) and then France, Holland, etc. (faience, 15th-16th c.).[23] Syrian, Persian and Ottoman potters also explored another route in relation to the inappropriately 'so-called' Egyptian "faience", as a sand-rich 'white' ceramic body which is better called stonepaste or fritware.[1,2,23,25-28] These ceramics can be produced with a colour palette larger than that of Chinese porcelain due to their lower temperature of firing. In particular, overglaze decors (*minai*, a Persian innovation) offered a very large chromatic palette. The top quality was achieved by Iznik (Turkey) potters during the 15th-16th centuries[23,26] and then by European potters (majolica, 17th/18th c. Rouen, Saint-Cloud, etc. soft-paste porcelains).[29] The Jesuits played a seminal role for the transfer of the European glazing technology to Japanese and Chinese potters during the 17th century, demonstrating that technological exchange is old and takes place in the reverse side rapidly.[30,31] The huge variety of materials (Table 4.1) represents a large variety of corrosion behaviour, but corrosion layers are always very small because ceramics and glasses are made of strong stable covalent bonds.

Roman glass is very similar to the soda-lime glass presently used for windows.[6,32] At that time, soda was mainly obtained from plant ashes in Levant. However, their importation had become difficult after the collapse of the Roman Empire. Then, potassium-rich local plants and wood ashes were used in Europe during the Middle Ages as well as in Great Britain up to the 18th century.[5,32] The selectivity of raw materials (replacement of river sand with pure quartz/silex pebbles) allowed the production of exquisite objects in Italy (*cristallo* and *Façon de Venise,* see Table 4.2) and the (re)discovery of new compositions in England by Ravenscroft in 1674, such as lead-based glass as a glass easy to shape with a high optical index.[6,32] K-containing glass was also being produced in Bohemia.[6,32]

Raw materials used in glassy artefacts determine minor phases and traces, hence the corrosion resistance. The higher alumina content, higher the chemical stability will be.[33,34] It is important to note that thermal expansion of inorganic materials ranges from ~10 to 150x10^{-7} K^{-1} and many phases exhibit huge thermal expansion jumps at phase transition (quartz at 573°C, cristobalite at 241/275°C, tridymite at 117°C and 163°C), which may induce stress and cracks[5,14,15,35]. However, a small compressive mismatch between the thermal expansions of the coating and the substrate is mandatory. If the thermal expansion mismatch between the substrate and the coating is too high, defects such as crazing (thermal expansion of the coating > that of the substrate) or peeling (vice versa) are observed (Fig. 2), promoting corrosion. Accordingly, food residues enter the cracks of the coating and a black network appears very clearly on ancient utensils. In that case, cleaning

with hot H_2O_2 or gently heating at ~600°C in air whitens the artefact. Consequently, potters and enamel makers experimented a huge variety of compositions, much larger than those used by glassmakers in order to prevent/control defects such as cracking, crazing, peeling, chipping and twitching.[5-8,16,35]

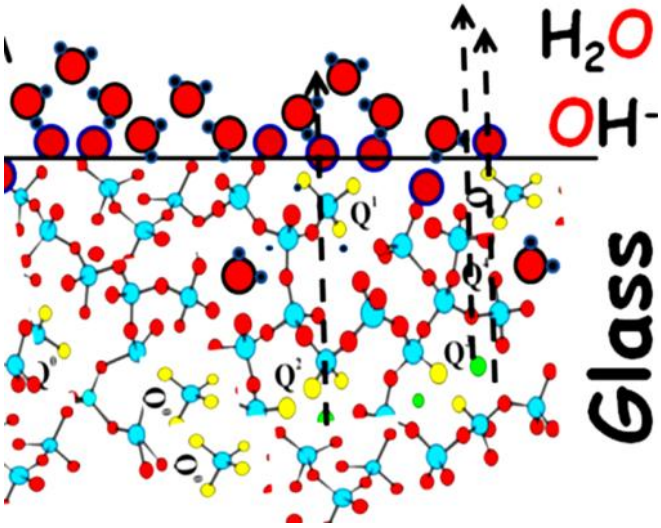

Figure 4.3 *Schema of glassy silicate network made of more or less connected SiO_4 tetrahedron (Q_0: isolated tetrahedron, Q_1: tetrahedron sharing a common oxygen atom with neighbouring tetrahedron, Q_2: tetrahedron sharing two oxygen atoms, etc.); other cations are distributed in between[38-40]; note the adsorption and diffusion of protonic species (proton, hydroxyl groups and water) in the near surface.*

4.3 Chemical and physical specificity of ceramics and glass

4.3.1 Preparation

The two preliminary steps in the preparation of glass, pottery and enamelled artefacts are the selection of the (natural) raw materials and their transformation into powder form by grinding or firing. Since grinding is a very energy consuming action, it had not been possible for a large quantity of rocks/minerals before the mastering of hydraulic energy was achieved at the end of the Middle Ages. Consequently, craftsmen prepared (ultra)fine powder (i.e. made of nanometric grains) by selecting naturally nanosized matter (clays, silts)[7,36] or by burning 'water-' or carbon-containing matter. Burning wood and plants gives nanosized alkali-rich ashes which can be used as flux or even directly as enamel/glaze precursor [6-8,14] while heating calcareous stone or shell gives chalk.[7] The sol-gel transition has been controlled by potters for millennia in order to prepare and shape clay-based mixtures.[7,36] Clays/marls are naturally made of nanometric slabs interacting with water (a few grams of bentonite clay gels a litre of water) and become very reactive during/after dehydroxylation/decarbonation (~600-800°C),[7,36] i.e. at the temperature of the formation of the first liquid phases. Firing atmosphere also controls the phase transformation, as in the case of the melting temperature of metal oxides (e.g. iron oxides) depending on the phase and speciation. For instance, the first liquid phase forms between FeO and alkali/earth alkali oxides, not with Fe_2O_3.[9] Consequently, sintering iron-rich clay is more efficient under reducing conditions. Diffusion of small (i.e. reduced) ions in solid and liquid states is faster and hence the firing atmosphere controls the diffusion rate of multivalent ions (Fe^{2+}/Fe^{3+}, Sn^{2+}/Sn^{4+}, Sb^{3+}/Sb^{5+}, Mn^{2+}/Mn^{5+}, etc.).[15,37] As a result, sintering and melting temperatures do not depend on the mean 'final' composition but on the composition of the ingredients, their grain size and distribution as well as the firing atmosphere. Typically, sintering of an inorganic ~10 µm grain mixture without liquid phase requires a temperature close to 0.8 x T_m (T_m: melting temperature) of the less refractory phase since the sintering temperature decreases with grain size and the increasing compaction in the green state. If the grain size is less than 0.1 µm (i.e. made of nanoparticles), sintering can occur at 0.5 x T_m. Enamel and glaze must completely melt to be homogeneous and

cover/wet the substrate. Perfect powdering of the enamel is thus mandatory.[16] Sintering conditions and chemical composition play an important role in the reactivity and corrosion resistance.

4.3.2 Compositions, phases and nanostructures

Table 1 shows representative compositions of the main types of pottery (terra cotta, faience, fritware, soft-paste porcelain, stoneware and porcelain) and of the associated glazes. Compositions of each group are in fact variable. **Table 2** shows representative glass compositions displaying less variety and five families can be recognized.[5,32] The formation of glassy silicates is associated with the easy polymerisation of SiO_4 tetrahedron and similar "molecular" entities such as PO_4, AlO_4, AlO_6, BO_3, BO_6, GeO_4, GeO_6, etc. XO_n units share 0 to n oxygen atoms, forming a more or less polymerized network (Fig. 3).[33,34,36-39] Elements such as Si, Ge, Al, P, B are thus called glass formers.

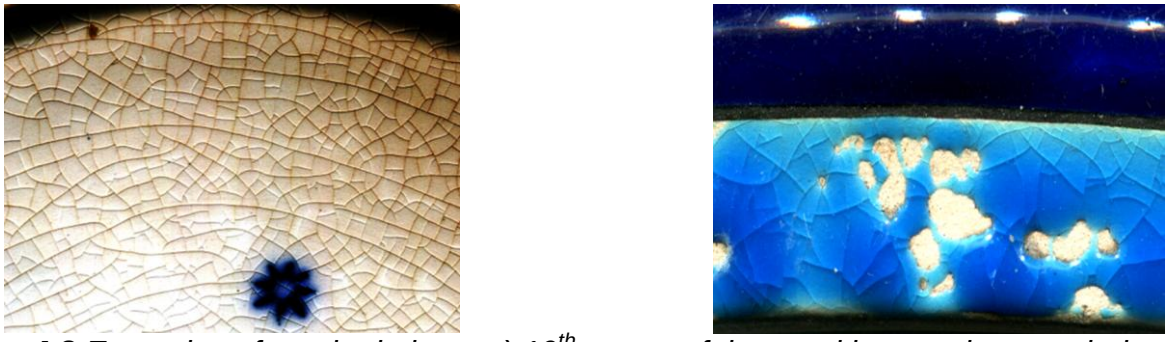

Figure 4.2 *Examples of cracked glaze: a) 19th century faience with a crack network due to the volume increase of the porous body with time; b) defective shard showing body areas without glaze and cracked glaze due to overgrinding of the glaze powder and thermal expansion mismatch.*

The melting temperature of SiO_2 is very high (>1700°C) and all the skill of glass- and enamel makers includes the replacement of strong covalent X-O bonds of glass former by weaker ionic ones, allowing the decrease of the melting temperature, viscosity as well as the control of wetting, colour and gloss. For instance, replacement of a Si^{4+} ion with four Na^+ ions replace four strong Si-O bonds with weaker Na..O bonds and hence induces a depolymerisation of the silicate network along with the decrease of the melting temperature and the viscosity but the increase of the thermal expansion[33,34,39,40] as well as the reactivity towards corrosion. The lowest strength of the ionic bonds will play a major role regarding chemical reactivity, ion exchange and degradation.[40,41] The diffusion coefficient of an alkali ion in silicates is many orders of magnitude higher than those of glass former ions and their ion exchange is easy.[33,34,40-41] This property has advantages (i.e. formation of lustre or yellow coloration of glass by silver and/or copper[37,42], surface hardening by ion exchange) as well as drawbacks (lixiviation and crumbling).[40,41]

Table 1: Examples of pottery body and glaze compositions

oxide	Terra cotta		faience		fritware		softpaste		stoneware		Hard paste	
	body	glaze	body	glaze	body	glaze	body	glaze	body	glaze	body	glaze
SiO_2	55.5	27.1	67.1	50.5	74.3			76	70.8	58		59
Al_2O_3	14.1	4.0	16.0	6.3	8.9			1.7	23.3	12		35
MgO[a]	8.0		1.0		0.6			1.4	0.2	2		
CaO[b]	6.3	2.1	13.2	1.3	7.8			12.6		20		0.3
K_2O[b]	0.2			4.9	1.0			3.1	3.5	1.5		4
Na_2O[b]	4.5			2.9	5.1			2.9	1.0	0.8		0.8
Fe_2O_3	8.8	3.1	2.0		0.2			0.7	0.5	2.2		0.3
TiO_2	1.5	0.2	0.6					0.1		0.8		0.1
P_2O_5										1.5		
PbO		62.7		23.3	0.4			1.1				
B_2O_3				10.8								
MnO_2	0.2											
Cl_2O					0.5							
	99.1	99.2	100	100	98.8			99.6	99.3	98.8		99.5

[a]in this example MgO is high but usually compensated by higher Alumina content.
[b]balance between alkali/earth alkali oxide is very variable as function of type of clay(s)

Table 2 : Examples of glass compositions

Oxide	Na-Ca glass		K-glass		cristallo	Façon de Venise	Cristal
SiO_2	63		50				
Al_2O_3	2		2.5				
MgO	0.2		5				
CaO	15		14.5				
K_2O	1.5		18.5				
Na_2O	18		2				
Fe_2O_3	0.2		1				
TiO_2							
P_2O_5			3.5				
PbO							
B_2O_3							
MnO_2	0.1		1				
	100		98				

4.3.3 Mechanical properties

Fracture of silicate materials, as in the case of most inorganic materials is brittle with very small strain (<2%) but high stress at rupture (0.1 to 0.5 GPa) due to their high Young modulus (>30 GPa).[33,34,43] Consequently, stress or choc at any scale may initiate a crack and the crack propagation can be very fast. Due to the covalent bonding, inorganic materials exhibit much higher compressive strength than tensile strength. Because of its thinness, a coating should not be put under tension but be gently compressed by the substrate to prevent spelling. Control of the thermal expansion mismatch between the glaze coating and the substrate as well as the over and under layers of enamel is thus a very important task for potters and enamellers. As long as the dilations are not appropriate, the enamel/glaze will poorly protect the porous substrate and degradation will be activated (except for porcelain and stoneware, the coating stability is always higher than that of the substrate). Heterogeneity, especially at (sub)micron scale is an advantage. For instance, when a propagating crack meets an inclusion, an interface or a pore, the stress intensity at the top of the crack decreases below the propagative value, due to the increase of the associated surface and the crack propagation stops: this is the composite effect.[44]

4.3.4. Chemical reactivity

Porosity (i.e. surface offered to contact reagents), composition (in particular flux to silica ratio) and grain size are prominent parameters controlling the resistance to corrosion. Unreacted and incompletely reacted grains also promote corrosion. The main reagent is water (rains, soil, sea, etc.).

4.4 Analytical procedures

General analytical techniques which are useful to study pieces or small artefacts at the laboratory (see e.g. ref. [32]) are not considered here. However, we should recall that a combination of methods is required to get a complete picture of a material, especially of its corroded layer(s). Corrosion products are generally poorly crystalline or amorphous. X-ray diffraction (XRD) hardly detects and identifies amorphous phases. On the contrary, Raman microspectroscopy and Fourier Transform Infrared spectroscopy (FTIR), especially using attenuated total reflectance (ATR) or diffuse reflectance (DRIFT) are well suited to identify surface layers. We will address sample preparation for laboratory analysis and specific techniques including measurements by mobile instruments, with an emphasis on calibration, quality and documentation.

4.4.1 Materials, techniques and characteristics

Fig. 1 shows the section of an enamelled pottery: the matter is heterogeneous; the body is covered with one (or many) glaze layer(s). Similar features are observed for all enamelled objects whatever the substrate is; ceramic, glass or metal. To improve the decor, an overglaze layer must be deposited on an already fired artefact and the new thermal treatment(s) must be made at a

temperature usually 100°C lower or more than that used for the previous one. This implies the addition of a higher amount of flux (alkalis, lead oxide, bismuth oxide, borax, etc.), thus leading to lower chemical resistance due to the more complete depolymerisation of the silicate network. The thickness of the glaze layer typically ranges between 50 µm and a few millimetres. The thin glaze layer observed on pottery is the ca. 20 µm 'slip' formed at the surface of red Roman *sigillata.*[45] A thin glaze layer is also obtained when the glazing is obtained by reaction-condensation with volatile ingredients (NaCl, PbO/PbS) put directly in the chimney to glaze stoneware or terra cotta, respectively. Lustre layer is also very thin (a few µm or less). [7,8,24] The thickest coatings (a few mm) are observed for celadons, a type of stoneware covered with a green to yellow opalescent glaze which imitates jade. [46]

In order to achieve a nice gloss and attach the coating perfectly to the substrate, the coating must be liquid with convenient viscosity and wetting angle at the top firing temperature.[14,16,35,47] Reactions will occur at the contact with the solid substrate such as partial dissolution and formation of new, glassy or crystalline phases and ion diffusion (Fig. 4). The analysis of interphase at high magnification thus provides much information.[17] However, the analysis of these different layers requires cutting (and polishing) the artefact or probing the matter progressively from the surface to the underlayer(s) up to the substrate. This is possible but not trivial up to a few tens/hundreds of nanometers, depending on the analytical instrument and the absorption of the beam. The profile study from the surface to the substrate is required to understand corrosion and degradation. Table 3 lists the methods of in-depth analysis and their characteristics. It should also be noted that the patina and/or (stable/active) corrosion films formed at the surface of metal artefacts are inorganic coatings made of metal oxides, sulphurs, sulphates, arsenates and their corrosion mechanisms are rather similar to those of glazes: the most aggressive medium is (acidic) water.

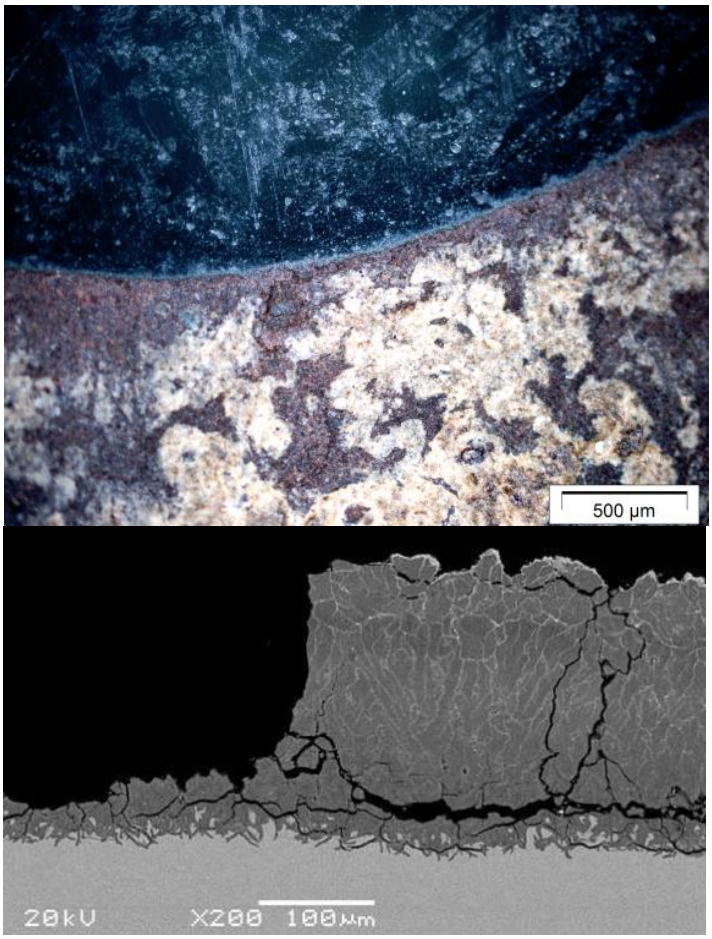

Figure 4.4 *Top) view from the top of a grisaille decor deposited on a piece of stained glass; note the white corrosion; bottom) SEM image of the polished section; note the crystals formed at the interface and the variety of cracks.*

Table 3: Standard characteristics of methods used for Cultural Heritage study.

Method	XRF	XRD	FTIR		ICPMS	LIBS	Raman	Accelerators		SEM-EDS
			Reflectance	ATR				Ion	Light (μXRF,μX)	
Probed area	cm^2	cm^2	cm^2	$<mm^2$	$>\mu m^2$	$>\mu m^2$	μm^2 to mm^2	$>\mu m^2$	$<\mu m^2$	$>\mu m^2$
penetration	Variable (f[element])	surface	Variable (f[wavenumber])			Controlled	Controlled & f(absorption)	Controlled		surface
Mapping	Yes	Yes		Yes			Yes	Yes	Yes	Yes
In-depth profile	variable	no	no	no	Yes	Yes	Yes	yes	variable	no
Sample preparation (Requirements)	no	(flat)	(flat & glossy)	(flat)	no	no	no			no

The calculation or even the estimation of the in-depth volume probed by a certain technique is far to be trivial, which explains the interest of analyzing a polished cross-section and not the external surface. For instance, penetration of the X-ray beam varies with energy and hence is not the same for all elements analyzed. Similarly, the in-depth volume probed by FTIR-ATR also depends on the wavenumber. Consequently, destructive techniques which require the preparation of a (polished) section are needed. Choice of the microscope objective determines the spot diameter but the in-depth focusing is strongly modified by light absorption, the optical index of the matter and the coupling with the spectrometer.[48] The advantage of micro-destructive methods such as Laser induced breakdown spectroscopy (LIBS)[49,50] and Laser ablation-inductively coupled plasma-mass spectroscopy (LA-ICP-MS)[51-53] is the progressive destruction-volatilisation of matter from the surface to the core which allows measuring the concentration profile and hence facilitating the comparison between the bulk and the corrosion layer composition. However, these techniques are risky for enamelled objects because the thermal stress at focus may induce cracks, peeling and even fracture. Raman microspectrometry performed on-site with mobile set-ups use much lower laser power whichguarantees a non-invasive procedure.[54] Additionally, rare ion beam instruments offering Proton induced gamma emission (PIGE), Proton induced X-ray emission (PIXE) and Rutherford back scattering (RBS) allow analysing profile composition (very) close to the surface. Mapping is also possible by these techniques.[55-57] Synchrotron light sources (and high power X-ray rotating sources) utilized in micro X-ray fluorescence (μXRF) (elemental composition), μXRD (phases) and micro X-ray absorption near edge structure spectroscopy (μXANES) (speciation) offer the best spatial resolution (micron or less). Mapping is again possible but estimation of the in-depth probed volume remains difficult and the analysis must be performed on polished or very flat sections.[58-63]

4.4.2 On-site analysis

Displacement of Cultural heritage objects out of secure preservation /exhibition places becomes more and more difficult at present and sampling is rarely possible. Many countries prohibit the exportation and transport of this type of objects. Four non-invasive techniques can be performed with commercially available mobile/portable/handheld instruments: Fibre optic reflectance spectroscopy (FORS) for chromophore and ion speciation identification,[64] FTIR in reflectance mode for chemical bond and phase identification,[65] Raman microspectroscopy (Fig. 5) for phase and nanostructure identification[25,39,54,66-68] and XRF for elemental composition (elements heavier than Na).[26,69-71] The composition shift induced by surface corrosion of glass must be corrected if the corroded layer is significant in comparison with the probed volume.[70] Home-made XRD instruments have been built but these are not used for pottery and glass. Recently, mobile (micro-destructive) LIBS set-ups have also become available for elemental composition measurements.[72,73] If sampling is possible, recent FTIR portable instruments can be coupled with a diamond ATR accessory.[74,75]

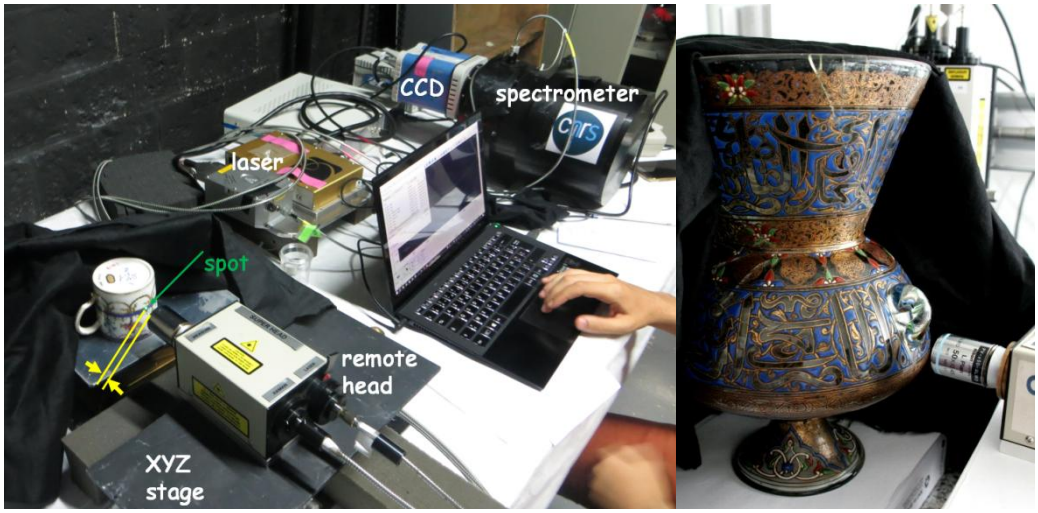

Figure 4.5 *Mobile Raman set-up installed in a museum storage room; note the ~15 mm distance between the front lens of the microscope objective and the artefact, allowing the analysis of the object with complex shape; the remote head connected by optic fibres to the laser and the spectrometer is put on a stage with controlled micrometer XYZ displacement. A black textile protects the eyes of the scientists and the measurement from the ambient light pollution.*

4.4.3 Specific analytical methods

Some analytical techniques are not currently used by larger academic community but are very popular in the professional ceramist community. For instance, measurements of porosity with Archimedes technique (comparison of the weights measured for the sample in dry, totally wet and immersed in water conditions),[14,76] pore size and distribution by N_2 (or Kr) gas adsorption (Brunauer-Emmett-Teller method) or liquid Hg intrusion under variable pressure,[77] thermal expansion by dilatometer[76,78] (Fig. 6) and micro-/nano- indentation by optical microscope coupled with a Vickers (isotropic pyramidal tip) or Knoop (anisotropic lozenge tip) diamond (or sapphire) indentor (Fig. 7).[40,79] Measurement of thermal expansion is among the most sensitive method to detect phase transformation (and the previous temperature used to fire the artefact) because the thermal expansion parameter measures the anharmonicity of the chemical bond potential.[80] The technique detects phase transition due to minor phases (cristobalite, trydimite, quartz, etc.) dispersed in a matrix and was long-time ago the main technique used by glassmakers and ceramists to optimize production[14,35] before the availability of advanced methods (Raman microspectroscopy, Castaing's electron probe microanalysis, etc.). For instance, Fig. 6 compares the thermal expansion measured on a non-corroded glass with that measured on a corroded glass. Absorbed and inserted protonic species (H_2O, H_3O^+, OH^-/H^+) are easily detected and quantified.

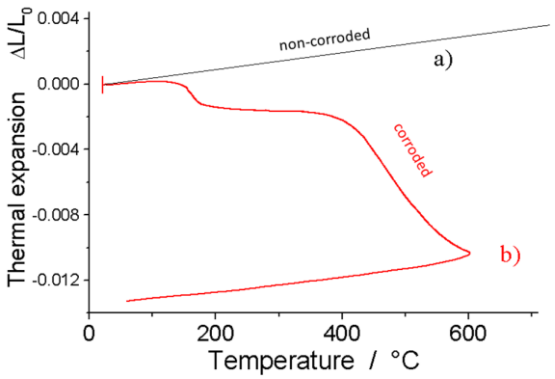

Figure 4.6 *Comparison of the thermal expansion measured on a non-corroded (a) and corroded (b) potash-lime glass showing the contraction due to the departure of adsorbed water layer (~180 °C) and of inserted protonic species above 400°C; on cooling the glass recovers the thermal expansion of the pristine state.*

4.5 Degradation

Table 4 lists representative examples of different types of corrosion.

Table 4: examples of degradation

Objects	Materials	Reactions	Refs	
Stained glass	K-glass	lixiviation	phc	
	grisaille	oxidation	etcheverry	
Reverse paintings on glass	Pigments & medium/varnish	reactions	Hahn	
Glass object	Cristallo	lixiviation	rodriges	
Glazed pottery	Lead-based enamel	dissolution		
	porcelain	lixiviation	kirmizi	
Cold painted enamels	Pigments & medium/varnisch		bottger	
Metal ware	Patina	reaction	phc	

4.5.1 Mechanisms

As noted supra, glassy artefacts produced at high temperature are very stable due to the nature of the chemical bond involved. There is a direct relationship between the bond strength and the melting temperature. Nevertheless, often neglected and very common, 'water' and dissolved ions can have very deleterious effects. However, the proton, the only ion without electron, is very small, between the size of an electron and that of lithium being the smallest 'standard' ion.[50,81] The proton can enter the electron shell of other species, inducing strong perturbation on neighbouring chemical bonds. It also diffuses very easily in oxide networks, even at ambient temperature.[80-82] Because of the similar ion diameter of K^+ and H_3O^+ ion, potassium glasses are the most sensitive to acidic corrosion. This explains the corrosion of many medieval glasses prepared using wood or plant ashes as a flux.[6,40,54,84-95] When the temperature increases, the departure of the proton generally leads to destruction, crumbling of the whole structure.[81] The reactions increase with the area exposed to reagents while porosity, and hence cracks amplify the reaction kinetics. Acidic water sources are common: meteoric water (sulphur-polluted water if coal combustion is used around and abroad due to the displacement of the clouds),[84] water in contact with humic acid in soil[90] and in the museum atmosphere, namely acids produced by wood cases.[96-99] Replacement of an atom by another with different size provokes huge dimension variation at the atomic scale and hence huge local stress. This leads to cracks, degradation of mechanical properties and even crazing and crumbling of the materials (Fig. 7). Obviously, compositional and environmental factors are very important.[100-103]

Change of the oxidation state also modifies the ion size, e.g. from 110 pm for Mn^{2+} ion (8-coordinate) to 39 pm for Mn^{7+} ion (4-coordinate). Ion oxidation is thus very detrimental (Fig. 3). For instance, the easy degradation of grisaille (the decor of stained glass panel, Figs 4 and 7) arises from its composition rich in lead oxide (sensitive to acidic corrosion), iron and manganese oxides (sensitive to oxidation).

Glaze and enamel coat a substrate. Bonding between the thin coating and the substrate occurs at high temperature when the substrate is solid but the coating is a viscous liquid in order to cover the surface and develop a chemical reaction (bonding) in between both materials and to keep a constant, controlled thickness of the coating as well. On cooling, the glassy coating becomes solid and both materials squeeze. Because the compressive mechanical strength of inorganic matter is much higher than the tensile one, the coating must be gently compressed to avoid scaling, peeling or partial delamination. This imposes the adaptation of the enamel/glaze composition according to the thermal expansion of the substrate[6,16] and this constraint explains the huge variety of compositions of glassy coatings. Faience and earthenware have porous bodies (porosity volume: 20% to 30%) which facilitate exchange and reaction with the environment. Reactions in fired ceramic bodies are always partial and unreacted/partially reacted relics of raw materials (quartz, feldspars and plagioclases, and more dangerously calcareous matter) are preserved, even in

stoneware and porcelains. In earthenware and terra cotta, artefacts fired at low temperature, the advancement of reactions between grains is minimal and limited to the periphery of grains. In that case, partially decomposed clays and carbonates can remain. Partially decomposed calcareous grains contain CaO phase which reacts with water (forming $Ca(OH)_2$ or even $CaCO_3$ again), inducing a huge volume expansion and cracks in the body, accelerating the phenomenon. This modifies the thermal expansion mismatch between the glaze and the body. Expansion of the porous body (faience, terra cotta) in humid atmosphere leads to cracking (Fig. 2) which can be (partially) cured by slow thermal treatment in oxidizing atmosphere at ~500°C.

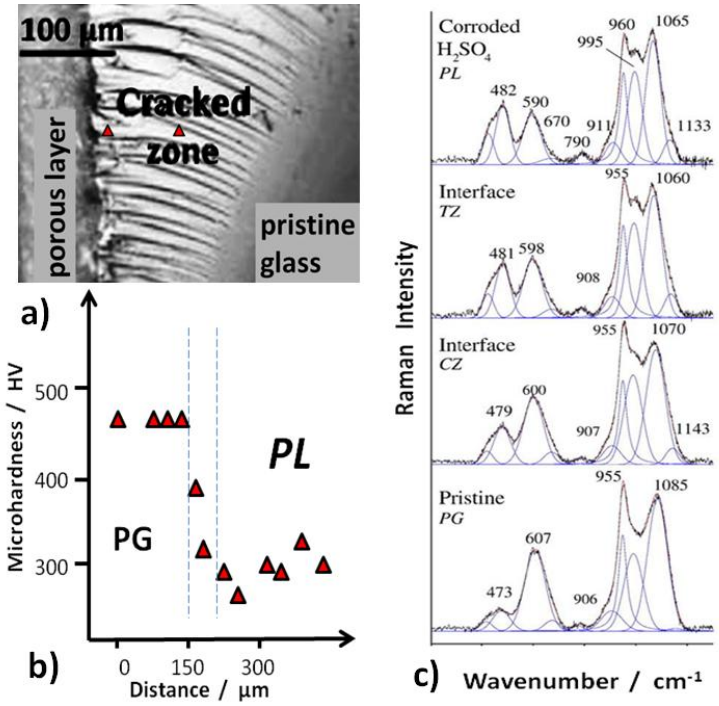

Figure 4.7 *Optical image of the fracture of acid corroded glass; a) showing transition cracked zone in-between the pristine non-corroded glass and the porous lixiviated layer; b) plot of the Vickers microhardness measured from the pristine glass to the porous layer; c) corresponding Raman spectra (after ref. [40]).*

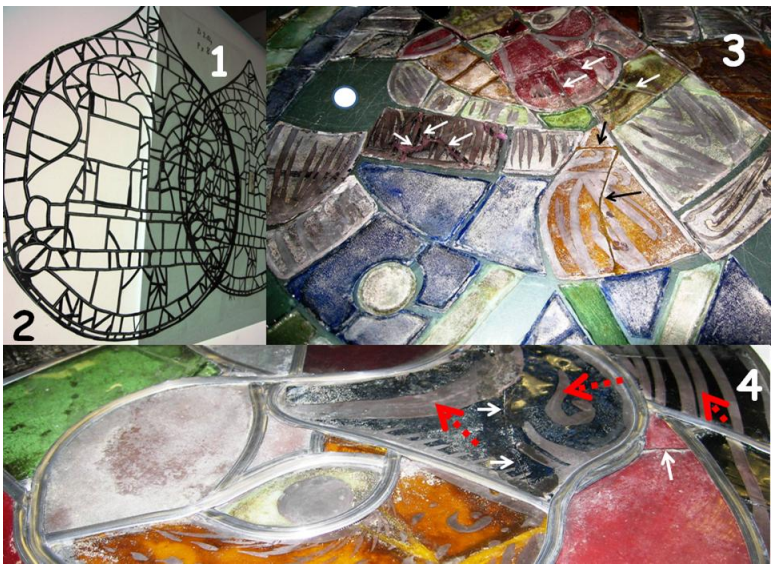

Figure 4.8 *Restoration of a medieval stained glass window; 1) drawing of the ancient lead frame; 2) building of the new frame; 3) each piece of glass is gently cleaned with appropriate chemicals, arrows indicate cracks filled with epoxy glue; 4) pieces are mounted in the new lead frame and then in the window panel support.*

4.5.2 Lixiviation and micro-cracking

Lixiviation rate has been measured for many glasses, for instance Rodrigues et al.[96] measured the rate ranging between 10 and 100 nm/year as a function of glass composition and ambient conditions, similar to that measured for obsidian. The corrosion rate of a single quartz crystal is about ten times lower but measurable with advanced nuclear techniques.[104] Acidic water is the most effective corrosive agent; lixiviation rates can reach about ten µm per hour in strong hot acids.[40,93] Lead-based glassy silicates are the most reactive (e.g. acetic acid from fruit juice easily dissolves lead-rich silicates) and hence are not authorized as culinary utensils for decades. In 'standard' conditions, the thickness of the corroded film at the surface of glass and enamelled object will increase by a maximum of a few µm per century and techniques of analysis must be local. Fig. 8 shows the restoration procedure of corroded stained glass: window panels are dismounted and cleaned gently to eliminate salts precipitated from the water containing lixiviated ions at the surface and in cracks and pits. The different degrees of corrosion are obvious: the most corroded glass pieces are those coloured in yellow by silver cementation[37] and the blue potassium-rich pieces.[40,93] The cementation process degrades the glass surface and increases its surface of reaction; the high potassium content accelerates the K^+-H_3O^+ ion exchange. Micro-analysis of 'natural' and accelerated aged glass pieces shows the different zones (Fig. 7): surface deposits when the reaction products are not/poorly eliminated by rain, porous layer of silicate "gel" formed by complete lixiviation, protonated and lixiviated glass, protonated (and cracked) and then pristine glass.[40] The modifications at the atomic level (Fig. 3) lead to huge volume variation and cracks. Micro-indentation (Fig. 7b) and Raman microspectroscopy (Fig. 7c) are very efficient to visualize these material modifications. The mechanical strength jumps down in the protonated and lixiviated layer. Raman microspectroscopy very well shows the modification of the silicate network under acidic corrosion. The intensity of Si-O bending components (500-600 cm^{-1} range) is strongly modified (formation of Si-O-H branch strongly modifies the SiO_4 symmetry and bond length). The downshift of the main stretching component (from ~1085 to 1065 cm^{-1}) arises from the lengthening of the Si-O bond due to the interaction between the proton and the oxygen atom.

However, the Raman spectrum of a glassy silicate is a very representative fingerprint of the SiO_4 network.[38,39] This approach has been used to compare Vietnamese celadon glaze from two kilns.[105] The silicate networks are different due to the small shifts in composition and firing temperature, hence the Raman fingerprint of the bending and stretching modes because of the different populations of Q_0 to Q_4 tetrahedral arrangements. The comparison of the bulk and the surface Raman fingerprints controls the preservation state.

4.5.3 Oxidation

An important degradation mechanism arises from ion oxidation. Glasses and ceramics are commonly fired under reducing atmosphere in order to control colour. For instance, whiteness of porcelain and colourlessness of glass impose iron traces with +2 oxidation state (Fe^{2+} in a silicate network gives a very weak blue colour). On the contrary, Fe^{3+} ion leads to the formation of yellow to amber colour (formation of Fe-S chromophore). Colouration with metal nanoparticles requires reduction through the help of go-between ions, fast diffusing multivalent small ions (Fe, Sn, etc.) which are reduced at the glass surface and develop redox action in the bulk after diffusion, hence control the speciation of colouring ions.[8,37,106,107] Grisaille, a painted decor of stained glass with high lead, iron and manganese composition, being fired at low temperature and highly porous degrades rapidly because of the oxidation of iron and manganese ions (Fig. 3).[93-96]

Regarding faience and terra cotta, the most encountered phases formed at the surface are carbonates, hydroxychlorides, sulphates and phosphates of lixiviated elements and/or of very reactive ones (lead). Contamination also occurs in marine and buried contexts. All these phases are easily detected by Raman or FTIR analysis. It should be noted that glass grains used as pigments in paintings are also subject to surface corrosion and fading.[108] Painting on pottery also often shows degradation.[109]

4.5.4 Biological alteration

Presence of calcium oxalate monohydrate (whedellite $CaC_2O_4 \cdot H_2O$, moolooite $CuC_2O_4 \cdot nH_2O$, etc.) is generally the signature of biochemical activity due to lichens, fungi, algae and bacteria or through chemical decomposition of organic materials namely proteins, oils, waxes, etc., leading to the formation of weak organic acids like oxalic acid. Raman detection of carotene (resonance for green laser excitation) is also the proof of bacterial activity.[110-115]

4.5.5 Cleaning, restoration and conservation

Conservation of glass and enamelled objects require special procedures (Fig. 8). The sensitivity of glass objects to mechanical shock is well known and the number of ancient objects preserved, especially enamelled glass, is very limited in comparison with pottery. As explained supra, enamelling creates a mechanical stress which can be partly reduced by thermal annealing. Thus, objects which were not well annealed will develop cracks in a few years.

A variety of glues and organic chemicals has been used to repair/protect ancient inorganic artefacts[116] and their disposal for new restoration requires identification in order to adapt the best cleaning procedure minimizing the use of hazardous chemicals. Comprehensive studies are limited and concern mainly other medical applications.[117-121]

Defects can be part of the aesthetic objective. *Raku* pottery is a typical art movement in Japan from the 17th century to the present times. [120] This movement what determines the aesthetic of contemporary art all around the world, searches to integrate defects due to hazards (bubbles, cracks, gloss and colour variation developed during firing) or defects intentionally provoked and corrected (fracture, see Fig. 9) as a part of the creative work. This movement has developed in opposition to the formal perfection achieved with Song white or monochrome porcelains and is linked to the first Vietnamese stoneware production. This art movement, also called *wabi sabi* (namely simple, natural and the wear of time, the decryption) was discovered by the Europeans by means of the Universal Exhibitions in the second half of the 19th century and has contributed to the craft movement as it still continues to inspire modern potters.[122]

Figure 4.9 *Raku pottery, intentionally broken and repaired with gold lake*

4.5.6 Degradation as a dating tool

5 Lixiviation of glassy silicates in contact with acidic water is well established and even measured for pure crystalline silica, in the form of quartz crystal.[104] The tiny corroded layer formed with time elapsed after the production date can be used to date a glassy artefact and in particular to identify a fake. This was first proposed theoretically a long time ago by Brill and Hood for glass[83] and Friedmann and Smith for obsidian.[123] However, it has only recently been demonstrated experimentally with the use of a high magnification microscope objective probing a few micron thick layer in which the near-surface layer hosting the protonic species is significant.[124] Fig. 10a' compares spectra recorded for a modern copy and an old celadon (13th century). Due to strong H-bonding, the signature of protonic species is broad and may have a complex shape but the contribution of stretching modes of the protonic species superimposes clearly over the fluorescence background. Spectrum measured on a modern

fake only shows the fluorescence background. Glaze composition and preservation conditions also drive the corrosion rate but the time elapsed is the dominant parameter for 'stable' (i.e. lead-poor) glaze. The surface corrosion decreases the optical quality of glass (and enamel) and hence the efficiency of light penetration which leads to the lowering of the scattered Raman signal collected. Consequently, the comparison of the signal intensity also allows relative dating, as demonstrated in the study of ancient stained glass windows (Fig. 10c').[54] The use of multivariate analysis easily visualizes the differences.

6

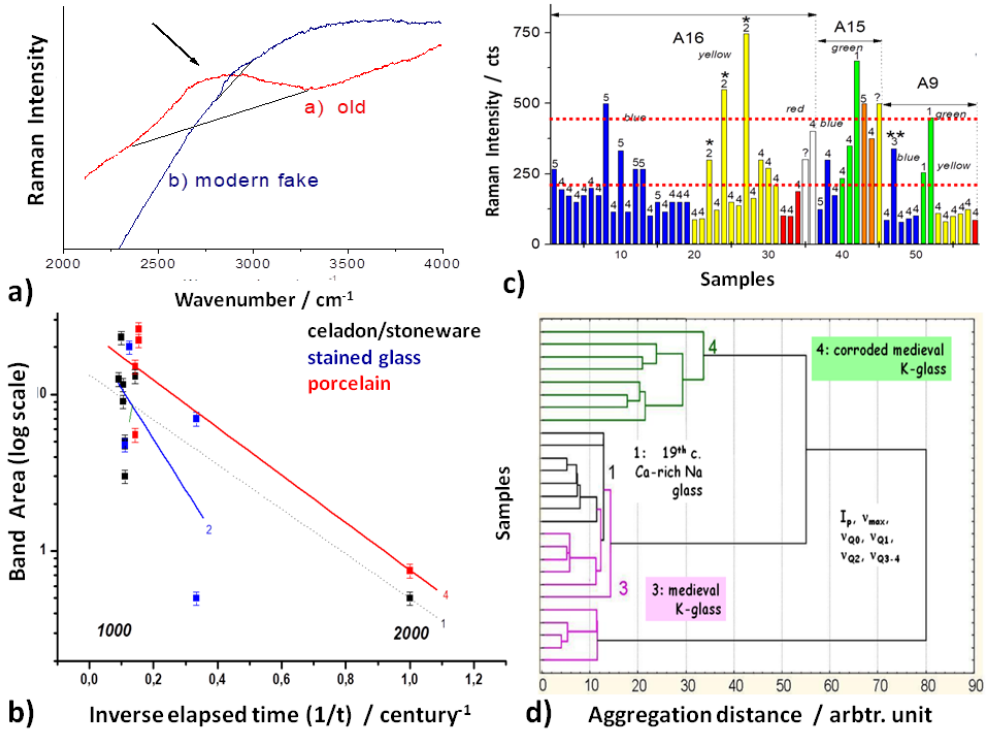

Figure 4.10 *Raman spectra a') of the protonic species inserted in the very surface of the glaze (extra bump contribution over the straight black line), (a) for a many century old artefact and (b) for a modern fake; b') comparison of the protonic band intensity versus elapsed time for series of samples (after [90]); c') comparison of the as-recorded Raman intensity on different blue, yellow, red, and green glass pieces of 3 different window panels (A15, A16 and A9) of Sainte-Chapelle church, Paris;[54] the different glass types (1 to 4) are noted; group identification can also be made using algorithms (Euclid distance classification using 6 variables: polymerisation index, peak and component wavenumber).*

7 Conclusions

Pottery and enamelled artefacts are very stable and preserved for millennia. However, the tiny corroded layer can now be studied by a variety of techniques. The most relevant studies have been devoted to stained glass windows due to their heavy exposition to aggressive meteoric water but the development of analytical techniques and the increase of attention to conservation problems may involve a further improvement of corrosion studies using surface analytical techniques.

Acknowledgements

Dr. Burcu Kırmızı is kindly acknowledged for the text editing.

References

1. W.D. Kingery ed., *Ancient Technology to Modern Science*, Ceramic and Civilization Series Vol. I, The American Ceramic Society, Columbus, 1984.

2. W.D. Kingery ed., *Technology and Style*, Ceramic and Civilization Series Vol. II, The American Ceramic Society, Columbus, 1986.
3. W.D. Kingery ed., *High Technology Ceramics –Past, Present, and Future. The Nature of Innovation and Change in Ceramic Technology*, Ceramic and Civilization Series Vol. III, The American Ceramic Society, Westerville, 1986.
4. P.E. McGovern, M.D. Notis and W.D. Kingery eds, *Cross-craft and Cross-Cultural Interactions in Ceramics*, Ceramic and Civilization SeriesVol. IV, The American Ceramic Society, Westerville, 1989.
5. Ph. Colomban, Glazes and enamels, in *Encyclopedia of Glass Science, Technology, History, and Culture*, ed. P. Richet, Wiley & Sons, New-York, 2019.
6. Ph. Colomban, Glass, Pottery and enamelled objects: identification of their technology and origin, in *Conservation Science – Heritage Materials*, ed. P. Garside and E. Richarson, The Royal Society of Chemistry, Cambridge, 2019.
7. Ph. Colomban, Natural nanosized raw materials and Sol-Gel technology : the base of pottery since millenniums in Nanosciences and Cultural Heritage, ed. Ph. Dillmann, L. Bellot-Gurlet and I. Nenner, Atlantis Press, 2016, p. 59-74.
8. Ph. Colomban, Nano-optique, céramiques et verres nano-structurés, des pratiques millénaires, in *Regards croisés: quand les sciences archéologiques rencontrent l'innovation*, eds M. Balasse and Ph. Dillmann Sciences Archéologiques Series, Editions des Archives Contemporaines, Paris, 2017, p. 99-122.
9. E.M. Levin, C.R. Robbins, and H.F. McMurdie, *Phase Diagrams for Ceramists*, The American Ceramic Society, 7 volumes, Westerville, 1964 -1991.
10. F. Koleini, L. C. Prinsloo, W. Biemond, Ph. Colomban, A.T. Ngo, J. C.A. Boeyens, and M. M. van der Ryst, *J. Cult. Herit.,* 2016, **19**, 435-444.
11. S. Chirikure, M. Manyanga, A.M. Pollard, F. Bandama, G. Mahachi, I. Pikirayi, *PLOS one,* **9[10]**, 2014, e111224.
12. S. Soriano, P. Villa, L. Wadley, *J. Archaeolog. Sci.* **34[5],** 2007, 681-703.
13. R. Crassard, M.D. Petraglia, A.G. Parker, A. Parton, R.G. Roberts, Z. Jacobs, A. Alsharekh, A. Al-Omari, P. Breeze, N.A. Drake, H.S. Groocutt, R. Jennings, E. Regagnon, C. Shipton, *PLOS one*, 2013, **8[7]**, e6861.
14. C.-A. Jouenne, *Céramique Générale* (2 volumes), Gauthier-Villars, 1960, Paris.
15. W.D. Kingery, H.K. Bowen and D.R. Uhlmann, *Introduction to Ceramics*, J. Wiley & Sons, New-York, 1976.
16. R.A. Eppler and D.R. Eppler, *Glazes and Glass Coatings*, The American Ceramic Society, Westerville, 2000.
17. M. Maggetti and A. d'Albis, *Eur. J. Mineral.*, 2017, **29[3]**, 347-367.
18. Ph. Colomban, M. Maggetti and A. d'Albis, *J. Eur. Ceram. Soc.,* 2018, **38[15]**, 5228-5233.
19. Ph. Colomban, G. Sagon and X.Faurel, *J. Raman Spectrosc*., 2001, **32[5]**, 351-360.
20. E. Neri, C. Morvan, Ph. Colomban, M. P. Guerra and V. Prigent, *Ceram. Int*. 2016, **42[16]**, 18859–18869.
21. E. Cooper,*Ten Thousand Years of Pottery* (4th ed.), University of Pennsylvania Press, Philadelphia, 2000.
22. Ph. Beaujard, *Les mondes de l'océan Indien. Vol. 1, De la formation de l'État au premier système monde afro-eurasien*. *Vol. 2, L'océan Indien, au cœur des globalisations de l'Ancien Monde (7e-15e siècles)*, Armand Colin, Paris, 2012.
23. J. Soustiel ed., *La Céramique Islamique - Le Guide du Connaisseur*, Office du Livre - Editions Vilo, Paris, 1985.
24. Ph. Colomban and C. Truong, *J. Raman Spectrosc*., 2004, **35[3]**, 195-207.
25. Ph. Colomban , V. Milande and L. Le Bihan, *J. Raman Spectrosc*., 2004, **35[]**, 527-535.
26. G. Şimşek, O. Ünsalan, K. Bayraktar and Ph. Colomban *Ceram. Int*., 2019, **45[1]**, 595-605.
27. M.S. Tite, *Archaeometry* 1989, **31[2]**, 115–132.
28. G. Şimşek, B. Demirsar Arlı, S. Kaya and Ph. Colomban, *J. Eur. Ceram. Soc*., 2019, **39[6]**, 2199-2209.
29. Ph. Colomban, T.-A. Lu, V. Milande, *Ceram. Int.,* 2018, **44[8]**, 9018-9026.

30. Ph. Colomban, Y. Zhang and B. Zhao, *Ceram. Int*., 2017, **43[]**, 12079-12088.
31. R. Montanari, M. F. Alberghina, A. Casanova Municchia, E. Massa, A. Pelagotti, C. Pelosi, S. Schiavone and A. Sodo, *J. Cult. Herit*., 2018, **32[]**, 232–237.
32. K. Janssens ed., *Modern Methods for Analysing Archaeological and Historical Glass*, *First Edition,* John Wiley & Sons Ltd, New-York, 2012.
33. J. Zarzycki, *Glasses and the Vitreous State*, Cambridge University Press, Cambridge, 1991.
34. H. Scholze, *Glass-Nature, Structure and Properties*, Springer-Verlag, New-York, 1991.
35. P. Munier, *Technologie des Faïences*, Gauthier-Villars, Paris, 1957.
36. Ph. Colomban, *Ceram. Int*., 1989, **15[],** 23-50.
37. Ph. Colomban, *J. Nano Research*, 2009, **8**, 109-132.
38. Ph. Colomban, *J. Non-Crystall. Solids*, 2003, **323[1-3]**, 180-187.
39. Ph. Colomban, in *Modern Methods for Analysing Archaeological and Historical Glass, First Edition*, K. Janssens ed., John Wiley & Sons Ltd, New-York, 2012, p. 275-300.
40. A. Tournié, P. Ricciardi and Ph. Colomban, *Solid State Ionics,* 2008, **179[38]**, 2142-2154.
41. T. Scanu, J. Guglielmi and Ph. Colomban, *Solid State Ionics*, 1994, **70/71**, 109-120.
42. Ph. Colomban and H. Schreiber, *J. Raman Spectrosc*., 2005, **36[9]**, 884-890.
43. P. Richet ed., *Encyclopedia of Glass Science, Technology, History, and Culture*, J. Wiley & Sons, 2019
44. K. K. Chawla, Composites Materials, Science and Engineering, 2nd Edition, Springer, New-York, 1998.
45. Ph. Sciau and Ph. Goudeau, *Eur. Phys. J. B*, 2015, **88**, 132. DOI: 10.1140/epjb/e2015-60253-8.
46. N. Wood, *Chinese Glazes,* University of Pennsylvania Press, Philadelphia, 1999.
47. M. Haussone, *Technologie Générale. Faïences, Grès, Porcelaines*, Bibliothèque Professionnelle Series, J.-B. Baillère & Fils, Paris, 1969.
48. G. Gouadec, L. Bellot-Gurlet, D. Baron and Ph. Colomban, in *Raman Imaging*, *Techniques & Applications,* ed. A. Zoubir, Springer Series in Optical Sciences, **Vol. 168**, Spinger, New-York, 2012, p. 85-118.
49. A.W. Miziolek, V. Palleschi and I. Schechte, *Laser Induced Breakdown Spectroscopy*, Cambridge, Cambridge University Press, 2006.
50. R. Gaudiuso, M. Dell'Aglio, O. De Pascale, G.S. Senesi, and A. De Giacomo, *Sensors*, 2010, **10[8]**, 7434-7468.
51. P. Degryse and J. Schneider, *J. Archaeol. Sci.,* 2008, **35[7]**, 1993-2000
52. P. Degryse, J. Henderson and G. Hodgins, *Isotopes in vitreous materials*, Leuven University Press, Leuven, 2009.
53. L. Dussubieux, C.M. Kusimba, V. Gogte, S.B. Kusimba, B. Gratuze and R. Oka, *Archaeometry*, 2008, **50**, 797-821
54. Ph. Colomban and A. Tournié, *J. Cult. Herit.,* 2007, **8[3]***,* 242-256.
55. G. Poupeau, F.-X. Le Bourdonnec, T. Carter, S. Delerue, M.S. Shackley, J.A. Barrat, S. Dubernet, P. Moretto, T. Calligaro, M. Milic and K. Kobayashi, *J. Archaeol. Sci*., 2010, **37[11]**, 2705-2720.
56. G. Padeletti, P. Fermo, A. Bouquillon, M. Aucouturier, F. Barbe, *Appl. Phys. A-Mater. Sci. & Process*., 2010, **100[3]**, 747-776.
57. M. Vilarigues and R.C. Da Silva, *Appl. Phys. A – Mater. Sci. & Process.*, 2004, **79[2]**, 373-378.
58. S. Coentro, L.C. Alves, C. Relvas, T. Ferreira, J. Mirao, J. Molera, T. Pradell, R.A.A. Trindade, R.C. Da Silva and V.S.F., Muralha, *Archaeometry,* 2017, **59[4]**, 667-684.
59. T. Pradell, G. Molina, J. Molera, J. Pla and A. Labrador, *Appl. Phys. A-Mater. Sci. & Process.,* 2013, **111[1]**, 121-127.
60. T. Pradell, J. Molera, N. Salvado and A. Labrador, *Appl. Phys. A-Mater. Sci. & Process.*, 2010, **99[2]**, 407-417.
61. Y. Leon, Ph. Sciau, M. Passelac, C. Sanchez, R. Sablayrolles, Ph. Goudeau and N. Tamura, *J. Anal. Atom. Spectrom.,* 2015, **30[3]**, 658-665.
62. T. Wang, T.Q. Zhu, Z.Y. Feng, B. Fayard, E. Pouyet, M. Cotte, W. De Nolf, M. Salome and

Ph. Sciau, *Anal. Chim. Acta*, 2016, **928**, 20-31.
63. G. Padeletti and P. Fermo, *Appl. Phys. A-Mater. Sci. & Process*., 2013, **113[4]**, 825-833.
64. C. Fornacelli, Ph. Colomban and I. Turbanti Memmi, *J. Raman Spectrosc*., 2015, **46[11],** 1129-1139.
65. Ph. Colomban and D. Mancini, *Arts*, 2013, ***2*[3]**, 111-123 doi:10.3390/arts2030111
66. Ph. Colomban, *J. Cult. Herit*., 2008, **9[Suppl.]**, e55-e60.
67. Ph. Colomban, *J. Raman Spectrosc*., 2012, **43[11]**, 1529-1535.
68. Ph. Colomban, *J. Raman Spectrosc*., 2018, **49[6]**, 921-634.
69. G. Şimşek, F. Casadio, Ph. Colomban, K. Faber, L. Bellot-Gurlet, G. Zelleke, V. Milande and E. Moinet, J. Am. Ceram. Soc. 2014, **97[9]**, 2745-2754.
70. F. Koleini, I. Pikirayi, A. Antonites and Ph. Colomban, *J. Archaeol. Sci. Rep*., 2017, **13**, 333-340.
71. M. Auxiliadora Gomez-Moron, P. Ortiz, J. Maria Martin Ramirez, R. Ortiz and J. Castaing, *Microchemical J*., 2016, **125**, 260-265.
72. I. Osticioli, J. Agresti, C. Fornacelli, I.T. Memi and S. Siano, *J. Anal. Atom. Spectrom*., 2012, **27[5]**, 827-833.
73. P. Panagiotis, A. Philippidis and D. Anglos, *Sprectrochim. Acta Part B-Atom. Spectrosc*., 2017, **137**, 93-100.
74. F. Rosi, R. Harig, C. Miliani, R. Braun, D. Sali, A. Daveri, B.G. Brunetti and A. Sgamellotti, Optics for Arts, Architecture, and Archaeology IV, eds L. Pezzati and P. Targowski, Proceedings of SPIE, 8790, 2013, UNSP 87900Q.
75. Ph. Colomban and L. Bellot-Gurlet, *L'Actualité Chimique,* 2017, **418-419**, 82-90.
76. Ph. Colomban, G. Sagon, C. Roche, D.N. Khoi and N.Q. Liem, *J. Cult. Herit.*, 2004, **5[2]**, 149-155.
77. S. Kramar and J. Lux, *Materiali in Technologije*, 2015, **49[4]**, 503-508.
78. N.Q. Liem, Ph. Colomban, G. Sagon, H.X. Tinh and T.B. Hoanh, *J. Cult. Herit.,* 2003, **4[3]**, 187-197.
79. Ph. Colomban and M. Havel, *J. Raman Spectrosc*., 2002, **33[10],** 789-795.
80. Ph. Colomban, *Fuel Cells* 2013, **13[1]**, 6-18.
81. Ph. Colomban Ed., Proton Conductors, Cambridge University Press, Cambridge, 1992.
82. R.H. Doremus, *J. Non-Crystall. Solids,* 1975, **19**, 137-144.
83. R.H. Brill and H.P. Hood, *Nature,* 1961, **189[4758],** 12-14.
84. R.G. Newton, *J. Glass Stud*., 1975, **17**, 161-168.
85. W.A. Lanford, K. Davis, P. Lamarche, T. Laursen, R. Groleau and R.H. Doremus, *J. Non-Crystall. Solids,* 1979, **33[2],** 249-266.
86. D.E. Clark, C.G. Pantano and L.L. Hench, *Corrosion of glass*, Book for industry, New-York, 1979.
87. M. Perez y Jorba, J.P. Dallas, C. Bauer, C. Bahezre and J.C. Martin, *J. Mater. Sci.,* 1980, **15[7]**, 1640-1647.
88. R.G. Newton, *Glass Technol*., 1985, **26**, 21-38.
89. S. Frank, *Glass and Archaeology*, Academic Press, London, 1982.
90. G.A. Cox and B.A. Ford, *J. Mater. Sci.,* 1993, **28[20]**, 5637-5647.
91. R.H. Doremus, *Glass Science, 2nd Edition*, J. Wiley & Sons, New-York, 1994.
92. M. Vilarigues and R.C. da Silva, *J. Non-Crystall. Solids,* 2006, **352[50-51]***,* 5368-5375.
93. Ph. Colomban, M.-P. Etcheverry, M. Asquier, M. Bounichou and A. Tounié, *J. Raman Spectrosc.*, 2006, **37[5]**, 614-626.
94. F. Farges, M.P. Etcheverry, A. Haddi, P. Trocellie, E. Curti and G. E. Brown, Jr., X-ray Absorption Fine Structure-XAFS13, AIP Conference Proceedings Book Series, eds B. Hedman and P. Painetta, 2007, **882**, 44-50.
95. M. Melcher, R. Wiesinger and M. Schreiner, *Acc. Chem. Res*., 2010, **43[6]**, 916-926.
96. A. Rodrigues, S. Fearn, T. Palomar and M. Vilarigues, *Corrosion Sci.,* 2018, **143**, 362–375.
97. C. Tschegg, *J. Archaeol. Sci*., 2009, **36[10]**, 2155-2161.
98. L. Robinet, C. Hall, K. Eremin, S. Fearn and J. Tate, *J. Non-Crystall. Solids*, 2009, **355**, 1479–1488.

99. L. Robinet, K. Eremin, B.C. del Arco and L.T. Gibson, J*. Raman Spectrosc*., 2004, **35[8-9]**, 662-670.
100. A. Baricza, B. Bajnoczi, M. Szabo, M. Toth, Z. Bendo and C. Szabo, *Carpathian J. Earth Env. Sci.*, 2016, **11[2]**, 449-462.
101. I. Garofano, M.D. Robador, J.L. Perez-Rodriguez, J. Castaing, C. Pacheco and A. Duran, *J. Eur. Cer. Soc.*, 2015, **35[15]**, 4307-4319.
102. T.-Q. Zhu, C.S. Wang, Z.W. Mao, L.X. Li and H. Huang, *Spectrosc. & Spectr. Anal*., 2010, **30[1]**, 266-269.
103. Q.J. He, S.L. Lu, Y.J. Pei, Y.L. Li and R.T. Zhao, *Stud. Conserv*., 2014, **59[Suppl. 1]**, S232-S233.
104. N.Q. Liem, N.T. Thanh and Ph. Colomban, *J. Raman Spectrosc*., 2002, **33[4]**, 287-294.
105. T. Calligaro, Y. Coquinot, I. Reiche, J. Castaing, J. Salomon, G. Ferrand and Y. Le Fur, *Appl. Phys. A-Mater.,* 2009, **94[4]**, 871-878.
106. Cl. Mirguet, P. Frederickx, Ph. Sciau and Ph. Colomban, *Phase Trans.*, 2008, **81[2-3]**, 253-266.
107. Ph. Sciau, L. Noé and Ph. Colomban, Ceram. Int. 2016, **42[14]**, 15349-15357.
108. C. Altavilla and E. Ciliberto, *Appl. Phys. A – Mater. Sci. & Process*., 2004, **79[2]**, 309-314.
109. C. Miliani, B. Doherty, A. Daveri, A. Loesch, H. Ulbricht, B.G. Brunetti and A. Sgamellotti, *Spectrochimica Acta Part A*, 2009, **73[4]**, 587.
110. L. Rampazzi, A. Andreotti, I. Bonaduce, M.P. Colombini, C. Colombo and L. Toniolo, *Talanta*, 2004, **63[4],** 967.
111. B. Doherty, M. Pamplona, C. Miliani, M. Matteini, A. Sgamellotti and B. Brunetti, *J. Cult. Herit.,* 2007, **8[2]**, 186.
112. K. Castro, A. Sarmiento, I. Martinez-Arkarazo, J.M. Madariaga and L.A. Fernandaz, *Anal. Chem*., 2008, **80[11],** 4103.
113. S. Rolleke, C. Gurtner, G. Pinar and W. Lubitz, O. Ciferri, P. Tiano and G. Mastromei Eds, Proc. International Conference on Microbiology and Conservation (ICMC), Florence, Italy, 17-19 June 1999, (Kluwer Academic/Plenum Publ., New York, 2000, p. 39-47.
114. M.L. Coutinho, A.Z. Miller, A. Phillip, J. Mirao, L. Dias, M.A. Rogerio-Candelera, C. Saiz-Jimenez, P.M. Martin-Sanchez, L. Cerqueira-Alves, M.F. Macedo, Biodetrioration of majolica glazed tiles by the fungus Devriesia imbrexigena, *Constr. & Build. Mater*. 212, **2019**, 49.
115. A. Rodrigues, S. Gutierrez-Patricio, A.Z. Miller, C. Saiz-Jimenez, R. Wiley, D. Nunes, M. Vilarigues, M.F. Macedo, Fungal biodeterioration of stained-glass windows, Inter. Biodeter. & Biodegrad. 90, 2014, 152.
116. M. Asquier, Ph. Colomban and V. Milande, *J. Raman Spectrosc.,* 2009, **40[11]**, 1641.
117. B.J. Nam and S.Y. Jang, J. Conserv. Sci. (보존과학회지), 2017, **33[6]**, 467.
118. M. Unal, P. Ramge and H.-C. Kuehne, Proc. 7th Asian Symposium on Polymers in Concrete, eds M.H. Özkul, H.N. Atahan, B.Y. Pekmezci and O. Şengül, 2012, p. 397.
119. I. Hermann and B.R. Lawn, *J. Biomed. Mater. Res. Part-B Appl. Biomat.,* 2007, **82B[1]**, 115.
120. P. Ceruti, F. Erovigni, F. Casella, S. Lombardo, *Minerva stomatologica*, 2005, **54[10]**, 531.
121. J. Kapolos, *Progr. Inorg. Coatings*, 2007, **59[2]**, 152.
122. Ph. Colomban ed., *Grès et Raku du Japon – Techniques décoratives et critères d'appréciation*, *Taoci, 3*, SFECO –Editions Findakly, Sully-sur-Loire, 2004.
123. I. Friedman, R.L. Smith, Science, 1959, **129[3358]**, 1285.
124. B. Kırmızı, S. Chen and Ph. Colomban, *J. Raman Spectrosc*., 2019, **50[5]**, 696.
125. S. Steger, D. Oesterle, R. Mayer, O. Hahn, S. Bretz, G. Geiger, *Archaeol. & Anthropol. Sci.*, 2019, **11[8]**, 4025.
126. Ph. Colomban, A. Tournié, Ph. Meynard, M. Maucuer, *J. Raman Spectrosc.* , 2012, **43[6]**, 799.

Table 4.1 Examples of pottery body and glaze compositions

oxide	terra cotta		faience		fritware		soft paste		stoneware		hard paste	
	body	*glaze*	*body*	*glaze*	*body*	*glaze*	*body*	*glaze*	*body*	*glaze*	*body*	*glaze*
SiO_2	55.5	27.1	67.1	55	74.3	52	73.5	76	70.8	58	69	59
Al_2O_3	14.1	4.0	16.0	6	8.9	0.5	2.5	1.7	23.3	12	20	35
MgO	8.0[a]		1.0		0.6	0.1	0.5	1.4	0.2	2	1	
CaO[b]	6.3	2.1	13.2	2	7.8	1	15	12.6		20	1.5	0.3
K_2O[b]	0.2			4.5	1.0	1	2	3.1	3.5	1.5	3	4
Na_2O[b]	4.5			2.5	5.1	14	5	2.9	1.0	0.8	3	0.8
Fe_2O_3	8.8	3.1	2.0		0.2	0.4	0.5	0.7	0.5	2.2	0.5	0.3
TiO_2	1.5	0.2	0.6					0.1		0.8	0.5	0.1
P_2O_5										1.5	(x)	
PbO		62.7		25	0.4	27	0.2	1.1				
MnO_2	0.2											
Cl_2O					0.5							
SnO_2				4		4	0.2					
	99.1	99.2	100	99	98.8	100	99.4	99.6	99.3	98.8	98.7	99.5

[a]in this example MgO is high but usually compensated by lower alumina content.
[b]balance between alkali/earth alkali oxide is very variable as a function of clay(s) type

Table 4.2 Examples of glass compositions.

oxide	Na-Ca glass	K glass	"*cristallo*"	"*Vitrum Blanchum*"	"*Façon de Venise*"	crystal	modern "float" glass	boro-silicate
SiO_2	60	50	70.5	66.5	65.5	58	67	80
Al_2O_3	2	2.5	0.7	1	1.5	0.1	1	2.5
MgO	0.2	5	1.5	3	3.5		3	
CaO	15	14.5	5	10	10		10	0.1
K_2O	1.5	18.5	3	3	0.2	13	3	0.3
Na_2O	18	2	17	14	13	3	15	4.5
Fe_2O_3	0.2	1	0.2	0.3	0.7	0.02	0.3	0.01
TiO_2			0.01	0.01	0.1			
P_2O_5		3.5	0.1	0.3	0.3		0.3	
PbO					0.1	22		
B_2O_3					0.1	0.5		12.3
MnO	0.1	1			1			
SnO_2								
As_2O_3						0.5		
a	98	98	98	98.1	96	98.1	96.6	99.6

[a]minor elements/oxides such as S, Cl, C, H, Zn, etc.

Table 3: Standard characteristics of the methods used for cultural heritage studies.

Method	XRF	XRD	FTIR		ICP-MS	LIBS	Raman	Accelerators		SEM-EDS
			Reflectance	ATR				Ion	Light: µ-XRF, µXRD	
Probed area	cm^2	cm^2	cm^2	$<mm^2$	$>\mu m^2$	$>\mu m^2$	μm^2 to mm^2	$>\mu m^2$	$<\mu m^2$	$>\mu m^2$
penetration	Variable (f[element])	surface	Variable (f[wavenumber])			Controlled	Controlled & f[absorption]	Controlled		surfaces
Mapping	Yes	Yes		Yes			Yes	Yes	Yes	Yes
In-depth profile	variable	no	no	No	Yes	Yes	Yes	yes	variable	no
Sample preparation (Requirements)	no	(flat)	(flat & glossy)	(flat)	no	no	no			no

Table 4: Examples of degradation and illustrating references

Objects	Materials	Reactions	Refs
Stained glass	glass	lixiviation	40,54,57,92-95,108
	grisaille	oxidation	93,94,95
	glass	biodegradation	115
Reverse paintings on glass	Pigments & medium/varnish	reactions	125
Glass object	Cristallo, Na-glass, etc.	lixiviation	96,98,99
(Glazed) pottery	Lead-based enamel	dissolution	97,100-103
	glaze	biodegradation	114
	porcelain	lixiviation	124
Cold painted enamels	Pigments & medium/varnish		109
Metal ware	Patina	reaction	126
Rock	marble	reaction	110,111